Quantum confinement effect in Si/Ge core-shell nanowires: First-principles calculations

Li Yang,[1,*] Ryza N. Musin,[2] Xiao-Qian Wang,[2] and M. Y. Chou[1]
[1]*School of Physics, Georgia Institute of Technology, Atlanta, Georgia 30332-0430, USA*
[2]*Department of Physics and Center for Functional Nanoscale Materials, Clark Atlanta University, Atlanta, Georgia 30314, USA*
(Received 20 February 2008; published 27 May 2008)

The electronic structure of Si/Ge core-shell nanowires along the [110] and [111] directions are studied with first-principles calculations. We identify the near-gap electronic states that are spatially separated within the core or the shell region, making it possible for a dopant to generate carriers in a different region. The confinement energies of these core and shell states provide an operational definition of the "band offset," which is not only size dependent but also component dependent. The optimal doping strategy in Si/Ge core-shell nanowires is proposed based on these energy results.

DOI: 10.1103/PhysRevB.77.195325 PACS number(s): 73.21.Hb, 71.15.Mb, 73.22.−f

I. INTRODUCTION

As the characteristic size of microelectronics approaches the submicron scale, building nanostructure-based electronic devices has become a subject of active research. The semiconductor nanowires (NW), as one of the prototypic nanostructures, exhibit unique electronic properties because of the quantum confinement effect in two of the three dimensions. They have been used to construct various devices such as the *p-n* junction diode,[1] the field effect transistor[2–4] (FET), the complimentary FET,[5] etc. As in typical devices, dopant impurities provide free carriers but at the same time, introduce defects, which scatter the carriers and limit the carrier mobility.

To eliminate this drawback, a doping strategy may be realized in the Si/Ge core-shell NWs, making use of the band offset between the core and shell states. It has been shown that a one-dimensional hole gas with ballistic transport can be produced in Si/Ge core-shell NWs, and that these core-shell NW-based devices exhibit competitive properties compared to the traditional ones but with a better transconductance and higher carrier mobility.[4] Under the right condition, the dopants introduced in the shell may inject free carriers into the core and vise versa. Since the impurities and free carriers are spatially separated, the scattering rate can be reduced and the carrier mobility improved.

The band offset in NWs is expected to be considerably different from that in bulk heterojunctions and to be strongly modified by the quantum confinement effect. Despite the experimental interests in the core-shell NWs,[4,6–9] a detailed theoretical study of the influence of quantum confinement on the band offset is still lacking. To analyze the experimental results in NWs, researchers usually use the band offsets from Si/Ge bulk heterojunctions[10,11] or superlattices,[12,13] which are not accurate in NWs because of the special geometry and reduced scales. In this work, we present a first-principles study of the electronic structure in Si/Ge core-shell NWs in order to provide a more accurate description of the effect of strong radial confinement on the energy levels of the carriers.

II. STRUCTURE AND CALCULATIONAL DETAILS

We consider Si/Ge core-shell NWs along the [110] and [111] directions in this study. The representative structures of the core-shell NWs are shown in Fig. 1. Summarized in Table I are the diameters and the numbers of atoms in one unit cell for the wires we have studied. The diameter of the NWs along the [110] direction is about 4.1 nm and up to 3.1 nm for [111] NWs. Based on the experimental results, all of the NWs under consideration have approximately a cylindrical shape. In order to study the intrinsic properties, the NW surfaces are passivated by hydrogen atoms. There are two factors affecting the confinement energy of the electronic states of interest in core-shell NWs. One is the component dependence and the other is the relative core-shell size. We present the results for [110] NWs to illustrate the dependence of the confinement energy on the core size. As shown in Table I, the five [110] NWs have different core size ratios with respect to a fixed total diameter. In addition, the confinement-energy dependence on the total diameter is discussed by considering four NWs along the [111] direction that have different total diameters but a fixed core size. The core material can be either silicon or germanium, while the shell material is the other element.

Our calculations are carried out using density functional theory within the local density approximation (LDA) and employing ultrasoft pseudopotentials with a plane-wave basis set. The Vienna *ab initio* simulation package[14] is used. Periodic-boundary conditions are employed in the *xy* plane with a supercell large enough to eliminate the interaction between neighboring wires in the study of one-particle ener-

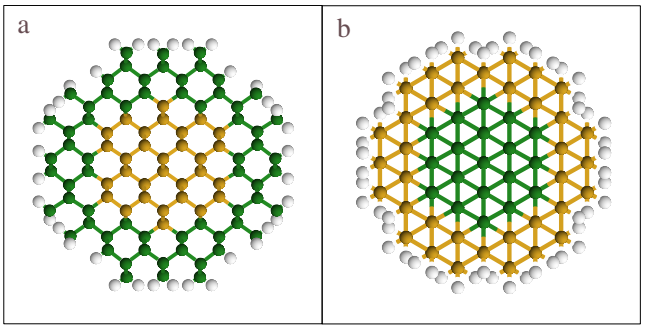

FIG. 1. (Color online) Top view of representative ball-and-stick models of hydrogen-passivated Si/Ge core-shell NWs along the (a) [110] and (b) [111] directions. Light spheres on the boundary are passivating hydrogen atoms.

TABLE I. Core-shell NWs investigated in this work. The numbers of Si/Ge atoms in the core and shell regions are shown. For NWs along the [110] direction, the total number of atoms in the NWs is fixed. For NWs along the [111] direction, we fix the core size and change the shell dimension. The diameter shown is approximate because the exact value changes slightly with the core/shell composition.

[110]	*d* (nm)	Core	Shell	[111]	*d* (nm)	Core	Shell
	4.1	30	232		1.8	62	48
	4.1	42	220		2.1	62	84
	4.1	62	200		2.6	62	180
	4.1	82	232		3.1	62	264
	4.1	122	140				

gies. The energy cutoff for the plane waves is in the range of 170–219 eV. The Monkhorst–Pack *k*-point mesh of $1\times1\times4$ or $1\times1\times6$ is found to provide sufficient accuracy in the Brillouin-zone integration. The structures are obtained by fully minimizing the forces and stress. Similar techniques have been used in recent studies of semiconductor nanowires.[15–19]

There is a mismatch of the silicon and germanium bulk lattice constant (4% difference), which introduces the strain in the interface of planar heterostructures. However, it would not be realistic to study core-shell nanowires with a chosen lattice constant instead of letting the atoms find their optimal positions. Therefore, the strain effect is included in our calculation by allowing all atoms in the nanowires to relax in order to minimize the total energy. This is different from the studies for planar heterostructures in which one can either grow a Si film on a Ge substrate or a Ge film on a Si substrate. Our relaxed structure shows that the average nearest-neighbor distance is between the values of bulk Si and bulk Ge, and both the Si and Ge parts are strained.

III. CONFINED ELECTRONIC STATES AND EFFECTIVE BAND OFFSETS

The typical electronic band dispersions in core-shell NWs along the [110] direction are shown in Fig. 2. One can see a clear feature inside the dashed frame that the energy level spacing near the band gap is larger than that away from the gap. It is interesting to note that the discrete set of states in the conduction band are more significant in the NW with a silicon core, while the discrete set of states in the valence bands are more noticeable in the NW with a germanium core. These discrete bands suggest additional confinement in the core or shell region for these core-shell NWs. In other words, there exist "band offsets" in these NWs that provide an additional geometrical confinement that can be tuned by varying the size and composition of the core-shell region. Similar results are also obtained in core-shell NWs along the [111] direction.

This confinement effect can be confirmed by examining the spatial distribution of these discrete states near the gap.

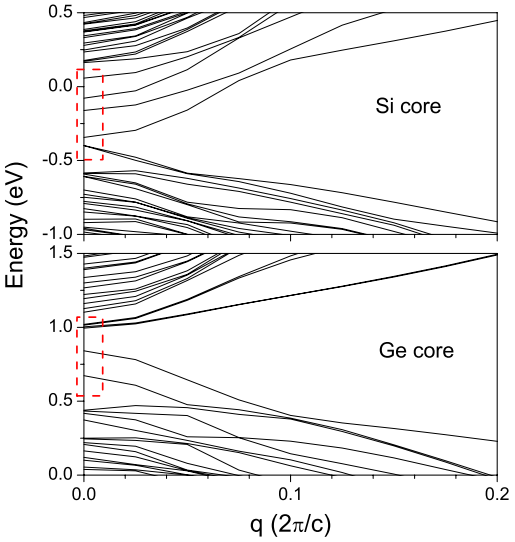

FIG. 2. (Color online) Band dispersions of core-shell [110] NWs with 42 atoms in the core and 220 atoms in the shell. The top figure is for the NW with a silicon core, and the bottom one is for the NW with a germanium core. The dashed frames indicate the energy regions of interest.

All of the NWs listed in Table I have a direct band gap at the zone center, hence, only the charge densities for states at the Γ point near the gap are presented below. The real-space charge density distributions, integrated along the axial direction within one unit cell, of representative states in NWs along the [110] and [111] directions are shown in Fig. 3. First, we focus on the states in germanium-core NWs. The [110] NW shown has 62 germanium atoms in the core and 200 silicon atoms in the shell. The state at the top of the valence bands, labeled as "VB550[110]" in Fig. 3, has a charge distribution mainly in the core region. In contrast, the state at the bottom of the conduction bands, labeled as "CB551[110]," has a charge distribution mainly in the shell region. This core-shell confinement feature can be easily concluded for these two states from the charge distribution. The asymmetry of the charge distribution arises from the fact that the *x* and *y* directions are not equivalent in [110] NWs and therefore have different effective masses, leading to different confinement extents in these two directions.

Moving down in energy from the valence band edge (band 550), the first valence state that is not confined in the core region is band 545, whose charge distribution, labeled as "VB545[110]" in Fig. 3, extends into the shell region and covers the whole NW. Moving up in energy from the conduction band edge (band 551), the first conduction state that is not confined in the shell is band 553 (CB553), with a charge distribution covering both the core and shell regions. We also plot a representative case in Fig. 3 for a [111] wire containing 62 silicon atoms in the core and 264 germanium atoms in the shell regions. The top of the valence band is band 697, which has charge mainly in the shell region. Below that, the first state that loses this confinement feature is band 690, as shown in Fig. 3. No clear confinement transition was found for the conduction bands in [111] NWs. The potential well seen by the conduction electrons in the core

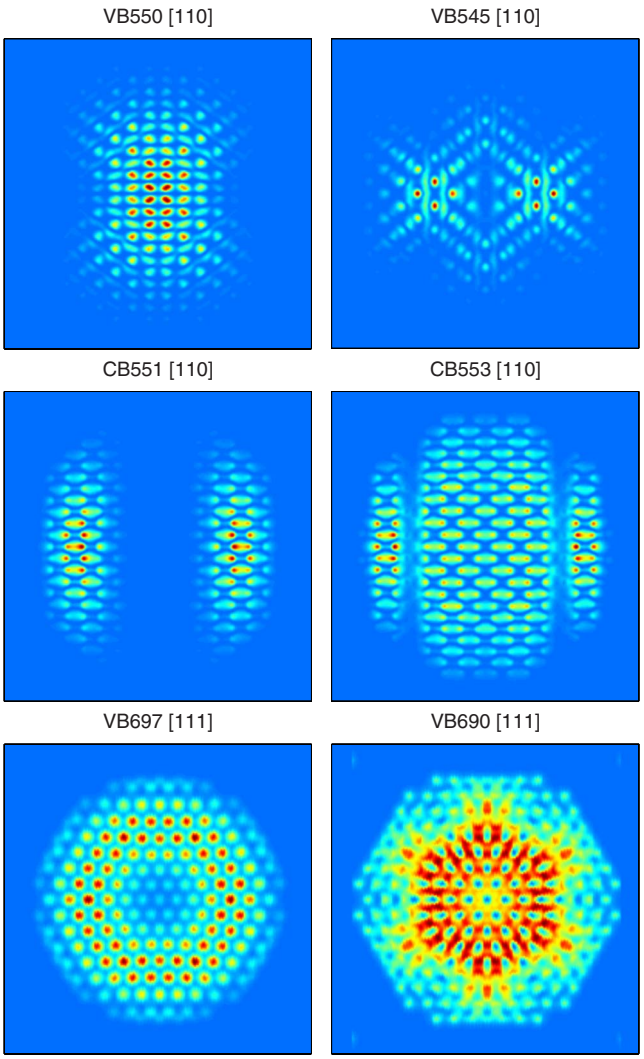

FIG. 3. (Color online) Charge distributions in the cross sections of core-shell NWs after integrating along the axis. Four states are shown for a [110] NW containing 62 germanium atoms in the core and 200 silicon atoms in the shell regions. Two states in the valence bands of a [111] NW containing 62 silicon atoms in the core and 264 germanium atoms in the shell region are also shown (see text).

region is simply not deep enough to create confined states.

After examining the charge distribution for all states at Γ near the gap, we find it possible to adopt a quantitative criterion to identify the confined states by calculating the total charge and the average charge density n within the core and shell regions, respectively. In the end, we assign a state to be confined in the core if $n(\text{core}) > 4n(\text{shell})$ and for small core cases if more than 70% of the charge is in the core. Similarly, a state is confined in the shell if $n(\text{shell}) > 4n(\text{core})$ or for small core cases if more than about 85% of the charge is in the shell region. By determining this energy range of confined states, one can come up with an operational definition of the effective band offset in these core-shell NWs. For example, we can take the energy difference of between VB550 and VB545 as the confinement energy for the [110] NW in Fig. 3, which provides an estimate of the effective band offset for the valence bands in this core-shell NW. A schematic is given in Fig. 4(b). In other words, the silicon

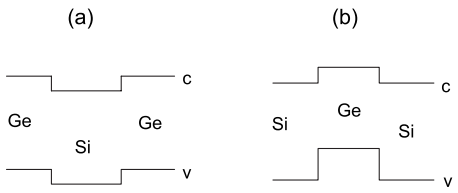

FIG. 4. Band lineups of Si/Ge core-shell NWs based on the analysis of electronic states near the gap. Schematic are shown for NWs with (a) a silicon core and a germanium shell and (b) a germanium core and a silicon shell.

shell region has a lower valence band edge than the germanium core region. Similarly, we can take the energy difference between CB551 and CB553 as an estimate of the confinement energy for the conduction states in this core-shell NW. The silicon shell region has a lower conduction band edge than the germanium core region. Because the core and shell regions are expected to induce different confinement effects, the confinement energies for the valence and conduction states do not have to be the same in core-shell NWs.

Based on what is outlined above, we obtain an estimate of the confinement energy for states near the gap in the Si/Ge core-shell NWs listed in Table I. The schematics are shown in Fig. 4 and the numerical results are presented in Fig. 5. The confinement energies for five [110] NWs with the same total number of Si/Ge atoms are plotted in Figs. 5(a) and 5(b)

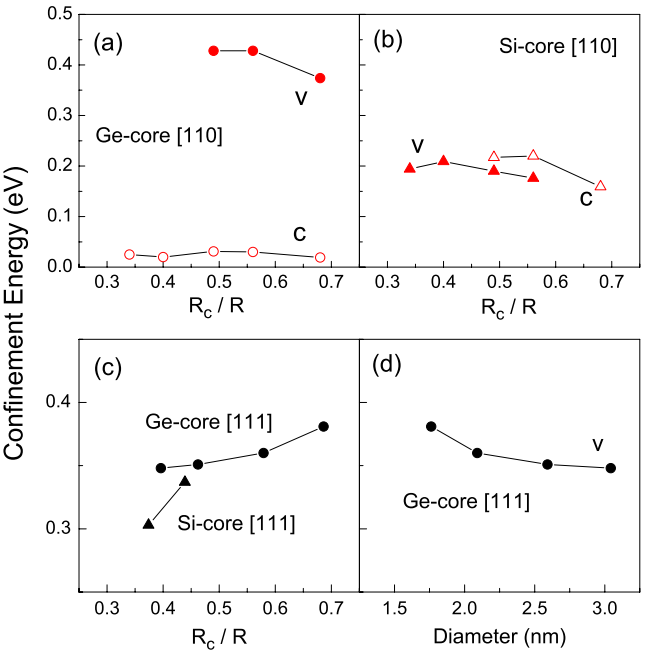

FIG. 5. (Color online) Confinement energy (as defined in the text) for the Si/Ge core-shell NWs along the [110] and [111] directions listed in Table I. The results for the valence (solid symbols) and conduction (open symbols) bands are labeled by "v" and "c," respectively. The results for [110] NWs with the same total number of Si/Ge atoms are plotted in (a) and (b) as a function of the ratio between the core radius R_c and the total radius R. The results for [111] NWs with a fixed core are plotted as a function of R_c/R in (c) and as a function of the total diameter in (d). Circles (triangles) denote the data for NWs with a germanium (silicon) core.

as a function of the ratio between the core radius (R_c) and total radius (R). All of the five NWs have a similar total radius, so the states that extend over the whole NW should be similar. The variation in the core size affects the confined states, thus, the confinement energies are expected to depend on the fraction of the core region in these NWs. However, the results in Figs. 5(a) and 5(b) do not suggest a straightforward scaling behavior: the energy values slightly vary as the size of the core changes. A few data points are missing in Figs. 5(a) and 5(b) for small core cases. These are associated with states confined in the core, which cannot be sustained if there is not a sizable core region. Of particular interest is the NWs with a germanium core in which the valence states have a significant confinement energy of the order of 0.4 eV, while the results for the conduction states are more than one order of magnitude smaller and are almost constant as the core size varies. In the latter case, the potential well seen by the conduction electrons in the core region is much shallower than that seen in the valence electrons.

The confinement energies for valence states in the [111] NWs listed in Table I are also plotted as a function of the ratio R_c/R in Fig. 5(c). The shell region decreases as R_c/R increases, making it difficult to sustain confined states in the shell. Therefore, no confined states in the shell are found for silicon-core [111] NWs with $R_c/R > 0.5$. For the [111] NWs with a fixed germanium core, the confined states in the core is expected to change little as the total wire radius varies. Hence, the confinement energy should depend on the energy of the states extended over the whole NW. The same set of data for the [111] NWs with a fixed germanium core is plotted in Fig. 5(d) as a function of the total diameter d. As expected, we see a decreasing confinement energy for the core states with increasing total diameter in a roughly d^{-2} fashion.

The schematic band lineup in Si/Ge core-shell NWs as shown in Fig. 4 indicates that these are type II band offsets, similar to those in the bulk Si/Ge superlattices and heterojunctions, although the values of the effective barrier height are modified in these NWs due to quantum confinement. In particular, we find that the confinement energy for valence states with a germanium core is consistently larger than other cases as long as there is a sufficient core region in order to confine these core states. Nevertheless, the possibility to generate states confined only in the core or shell region exists for a variety of configurations and R_c/R ratios, as shown in Fig. 5. In many cases, the confinement energy is significant compared to the thermal energy.

The current results suggest a doping strategy in these Ge/Si core-shell NWs. For the silicon-core [110] NWs, either n- or p-type doping can be considered. For the n-type (p-type) doping, it is possible to confine the electrons (holes) in the core (shell), therefore, the dopant impurity should be placed in the shell (core). For the germanium-core [110] and [111] NWs, the confinement energy for the holes in the core is optimal, therefore, the p-type dopants should be introduced in the shell region. This is consistent with a recently published experiment,[4] although the self-doping method was used to obtain free carriers.

It is well known that LDA calculations underestimate the band gap values. This can be corrected by evaluating the self-energy for the quasiparticles using the many-body perturbation theory with Green's function method within the so-called GW approximation.[20] Up to date, GW calculations have been performed only for small NWs with a diameter up to 2.0 nm[15,19,21] in which self-energy corrections are shown to be significant. The NWs studied here are too large for an accurate quasiparticle calculation with the current computational capacity. However, the confinement energy considered in this work is obtained by taking the energy difference between two valence or two conduction states instead of the energy difference across the gap. Therefore, the error due to the self-energy correction in the confinement energy discussed above is expected to be insignificant compared to that for the band gap.

IV. SUMMARY

In conclusion, we have performed first-principles calculations on Si/Ge core-shell nanowires along the [110] and [111] directions with a focus on the electronic states confined in either the core or the shell region. The results are obtained for nanowires with different size and composition. The spatial confinement in these Si/Ge core-shell nanowires is found to be consistent with a type II band offset. The values of the confinement energy are calculated for both the valence and conduction states. The calculated results suggest the doping strategy for different types of Si/Ge core-shell nanowires.

ACKNOWLEDGMENTS

This work is supported by the National Science Foundation (Grant No. DMR-02-05328) and U.S. Department of Energy (Grant No. DE-AC03-76SF00098). We acknowledge the use of computational resources at the San Diego Supercomputer Center (SDSC) and the National Energy Research Scientific Computing Center (NERSC).

*Present Address: Department of Physics, University of California at Berkeley, Berkeley, California 94720, USA.

[1] X. Duan *et al.*, Nature (London) **409**, 66 (2001).
[2] L. J. Lauhon *et al.*, Nature (London) **420**, 57 (2002).
[3] Y. Cui *et al.*, Nano Lett. **3**, 149 (2003).
[4] W. Lu *et al.*, Proc. Natl. Acad. Sci. U.S.A. **102**, 10046 (2005); J. Xiang *et al.*, Nature (London) **441**, 489 (2006).
[5] A. B. Greytak *et al.*, Appl. Phys. Lett. **84**, 4176 (2004).
[6] M. S. Gudiksen *et al.*, Nature (London) **415**, 617 (2002).
[7] J. Noborisaka *et al.*, Appl. Phys. Lett. **87**, 093109 (2005).
[8] M. T. Björk *et al.*, Appl. Phys. Lett. **80**, 1058 (2002).
[9] M. M. Glazov, P. S. Alekseev, M. A. Odnoblyudov, V. M. Chistyakov, S. A. Tarasenko, and I. N. Yassievich, Phys. Rev. B **71**, 155313 (2005).

[10] C. G. Van de Walle and R. M. Martin, Phys. Rev. B **34**, 5621 (1986).
[11] F. Schäffler, Semicond. Sci. Technol. **12**, 1515 (1997).
[12] C. Tserbak and G. Theodorou, Semicond. Sci. Technol. **10**, 1604 (1995).
[13] C. L. Chang *et al.*, Appl. Phys. Lett. **73**, 3568 (1998).
[14] G. Kresse and J. Furthmuller, Phys. Rev. B **54**, 11169 (1996); Comput. Mater. Sci. **6**, 15 (1996).
[15] X. Zhao, C. M. Wei, L. Yang, and M. Y. Chou, Phys. Rev. Lett. **92**, 236805 (2004).
[16] R. N. Musin and X.-Q. Wang, Phys. Rev. B **71**, 155318 (2005).
[17] R. Rurali and N. Lorente, Phys. Rev. Lett. **94**, 026805 (2005).
[18] T. Vo, A. J. Williamson, and G. Galli, Phys. Rev. B **74**, 045116 (2006).
[19] M. Bruno, M. Palummo, R. DelSole, V. Olevano, A. N. Kholod, and S. Ossicini, Phys. Rev. B **72**, 153310 (2005); M. Bruno, M. Palummo, A. Marini, R. DelSole, and S. Ossicini, Phys. Rev. Lett. **98**, 036807 (2007).
[20] M. S. Hybertsen and S. G. Louie, Phys. Rev. B **34**, 5390 (1986), and references therein.
[21] Jia-An Yan, Li Yang, and M. Y. Chou, Phys. Rev. B **76**, 115319 (2007).